18TH WORLD CONFERENCE ON EARTHQUAKE ENGINEERING
WCEE2024
MILAN

MILAN, ITALY
30TH JUNE - 5TH JULY 2024

www.wcee2024.it

INVESTIGATION OF STONE MASONRY CONSTRUCTION TECHNIQUES AND MATERIAL PROPERTIES IN HATAY AND OSMANIYE AFTER THE 2023 TURKEY-SYRIA EARTHQUAKES

B. Bozyigit[1,2], A. Özdemir[3], K. Donmez[4], K.D. Dalgic[5], E. Durgut[6], C. Yesilyurt[5], Y. Dizgin[7], C. Yıldeniz[8], M. Ispir[6], I. Bedirhanoglu[7], Y.D. Aktas[4], S. Acikgoz[1]

[1] University of Oxford, Oxford, UK, baran.bozyigit@deu.edu.tr; baran.bozyigit@eng.ox.ac.uk

[2] Dokuz Eylul University, Izmir, Turkey

[3] Gazi University, Ankara, Turkey

[4] University College London, London, UK

[5] Izmir Institute of Technology, Izmir, Turkey

[6] Istanbul Technical University, Istanbul, Turkey

[7] Dicle University, Diyarbakir, Turkey

[8] Chamber of Architects, Diyarbakir, Turkey

Abstract: *The eleven Turkish provinces affected by the 2023 Turkey-Syria earthquakes featured historic cities which are home to numerous stone masonry structures. Scientific evaluations of the earthquake response of these structures requires knowledge of the construction techniques as well as the mechanical properties of the constituent masonry materials (stone and mortar). However, limited research has been conducted on these aspects to date. To address this research gap, a post-earthquake field study was conducted on monumental structures located in two of the affected provinces (Hatay and Osmaniye). The paper first provides a survey of damage observations from the field; these highlight the significant role of masonry disaggregation in collapse mechanisms. To understand the reasons for disaggregation failures, construction techniques are investigated systematically using the Masonry Quality Index (MQI). The use of Ultrasonic Pulse Velocity, Schmidt Rebound Hammer and Mortar Penetrometer devices to quantify mechanical properties of stone and mortar is then presented. Examples are provided to demonstrate how the construction technique and material property data informs our understanding of damage mechanisms.*

1. Introduction

The province of Kahramanmaraş (Turkey) was hit by two earthquakes on 6 February 2023. The epicentre of first earthquake (moment magnitude (M_w) of 7.8) was in Pazarcık while the second earthquake occurred in Elbistan (M_w of 7.5). A major aftershock occurred in the province of Hatay on 20 February 2023 with an epicentre at Uzunbağ (M_w of 6.3) (USGS, 2023). 19,284 buildings collapsed in ten cities while more than 370,000 buildings were reported as damaged. The number of fatalities and injuries were reported as more than 50,000 and 100,000, respectively (Ozkula et al., 2023).

The neighbouring provinces of Hatay and Osmaniye have a significant historic stone masonry building stock which was affected by the 2023 Turkey-Syria earthquakes. Monumental buildings in these provinces suffered

damage. Some iconic buildings, such as the Habib-i Neccar mosque, experienced partial or total collapse. There is limited research in the scientific literature concerning the construction techniques and material properties of masonry buildings in these provinces. Without this information, it is difficult to carry out a scientific evaluation of the damage experienced by the buildings. To this end, this paper first surveys the damage (Section 2) and then evaluates the construction techniques (Section 3) and mechanical properties (Section 4) of 29 monumental historic masonry buildings. Section 5 explores correlations between observed damage, construction quality and material properties to inform a better understanding of failure mechanisms.

2. Building damage survey

29 stone masonry buildings consisting of monumental churches (C), mosques (M), public (P) and residential (R) buildings were investigated by the authors in the aftermath of the earthquakes. The investigated buildings are listed in Table 1 with an ID, wall construction type, district and resultant peak ground acceleration (PGA) values from the nearest strong-ground motion station (AFAD, 2023). The distance of nearest stations to the investigated buildings varies between 0.7 km (for M8) and 11.6 km (for M6) while the average building-to-station distance is 3.2 km. The Elbistan event (M_w = 7.5) is not considered as it is far away from the structures.

The masonry wall types of RSM and ISM in Table 1 represent regular stone masonry and irregular stone masonry. The RSM classification refers to buildings which have an external façade constructed from cut-stones. This classification includes multi-leaf masonry (MLM) walls with double or triple leaf masonry. The ISM classification is assigned to the rest of the buildings; the stone layout in these buildings is typically irregular and stone units are of variable non-rectangular shape and size.

Table 1. ID, location, district and resultant PGA data for the investigated buildings

Building name	ID (wall construction)	District	Resultant PGA (*g*)		Disaggregation
			6 Feb 2023 Pazarcık (M_w=7.8)	20 Feb 2023 Uzunbağ (M_w=6.3)	
Surp Karasun Manuk Church	C1 (RSM)	İskenderun	0.33	0.12	No
St. Nicholas Orthodox Church	C2 (ISM)	İskenderun	0.33	0.12	Yes
Latin Catholic Church	C3 (RSM)	İskenderun	0.33	0.12	Yes
Syriac Catholic Church	C4 (ISM)	İskenderun	0.33	0.12	No
Batıayaz Armenian Church	C5 (RSM)	Samandağ	0.26	0.22	No
The Virgin Mary Samandağ Orthodox Church	C6 (ISM)	Samandağ	0.26	0.22	Yes
St. Ilyas Orthodox Church	C7 (ISM)	Samandağ	0.26	0.22	Yes
St George Sarılar Orthodox Church	C8 (ISM)	Altınözü	0.54	0.33	Yes
The Virgin Mary Tokaçlı Orthodox Church	C9 (ISM)	Altınözü	0.54	0.33	Yes
St George Iskenderun Orthodox Church	C10 (n/a)*	İskenderun	0.33	0.12	No
Habib-i Neccar Mosque	M1 (RSM)	Antakya	0.58	0.54	Yes
Sarımiye Mosque	M2 (RSM)	Antakya	0.42	0.54	No
Şeyh Ali Mosque	M3 (RSM)	Antakya	0.58	0.54	Yes
Kurşunlu Han Mosque	M4 (RSM)	Antakya	0.58	0.54	Yes
Enverül Hamit Mosque	M5 (ISM)	Merkez	0.19	0.04	Yes
Ağcabey Mosque	M6 (RSM)	Bahçe	0.29	0.02	No
Ala Mosque	M7 (RSM)	Kadirli	0.2	0.01	No
Hamidiye Mosque	M8 (RSM)	Kadirli	0.2	0.01	No
Hatay Metropolitan Municipality Building	P1 (RSM)	Antakya	0.66	0.54	Yes
Mithatpaşa Primary School	P2 (ISM)	İskenderun	0.33	0.12	Yes
Yedi Ocak Primary School	P3 (ISM)	Merkez	0.19	0.04	Yes
Antakya High School	P4 (RSM)	Antakya	0.66	0.54	Yes

Iskenderun High School	P5 (ISM)	İskenderun	0.33	0.12	Yes
Olive Museum	P6 (RSM)	Altınözü	0.54	0.33	Yes
Gali Mansion-I	R1 (RSM)	Antakya	0.58	0.54	Yes
Gali Mansion-II	R2 (RSM)	Antakya	0.58	0.54	Yes
Hıdırbey Gastronomy House	R3 (RSM)	Samandağ	0.26	0.22	No
Vakıflı No.2 House	R4 (RSM)	Samandağ	0.26	0.22	Yes
Old English School	R5 (RSM)	Samandağ	0.26	0.22	Yes

**The wall construction type unknown as wall surfaces/cross-sections unexposed.*

A damage level was assigned to each building. For this purpose, damage grades (DGs) from EMS-98 (Mavroulis et al. 2019) were used. Figure 1 represents the DG definitions of EMS-98 (Grünthal and Levret, 1998). Although DG definitions in Figure 1 consider damage in both structural and non-structural elements in the classification, damage assignments in this study were done considering structural damage to walls only. This enabled consistent comparisons between different building typologies which may have different structural and non-structural components. For instance, arched porch structures, domes or minarets in mosques were not considered in the DG assignment; damage was evaluated solely from the structural walls. This enabled like for like comparisons with damage in church, public and residential building walls.

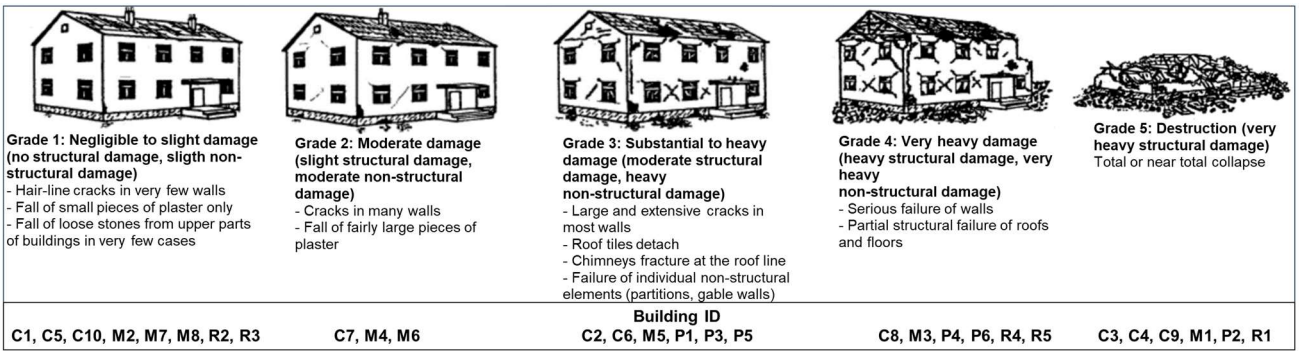

Figure 1. EMS-98 damage classifications (Grünthal and Levret, 1998) *and assignment of DGs to the investigated buildings*

Figures 2a-b show the relationship between the maximum resultant PGA and the DG for each building. There is no obvious relationship between the seismic demands and damage. In Figure 2a, individual markers are coloured according to the use of the buildings (e.g. church). Although the public buildings appear to be associated with high DGs (3-5), the sample size is small and no clear trend can be established between damage and building use.

In Figure 2b, markers are coloured according to the wall construction type (e.g. RSM or ISM). In general, ISM buildings appear to have experienced lower seismic demands and high damage. Except for one, all ISM buildings are assigned DG3 or more. This observation is consistent with the well-known vulnerability of this construction type to earthquakes.

In Figure 2b, there is a wider range of seismic demands for RSM buildings. Half of the 18 RSM buildings were subjected to resultant PGAs higher than 0.5*g* and experienced damage ranging from DG1 to 5. The remaining 9 RSM buildings were subjected to resultant PGA values lower than 0.4*g*. These buildings were classified either with DG1-2 (up to moderate damage), DG4 (heavy damage) or DG5 (near or full collapse). In particular, the building R4 (highlighted in Figure 2b) experienced out-of-plane collapse while R3 (also highlighted in Figure 2b) showed no signs of damage under similar seismic demands. It is noteworthy that the buildings R3 and R4 are two-storey residential buildings, with similar structural configurations.

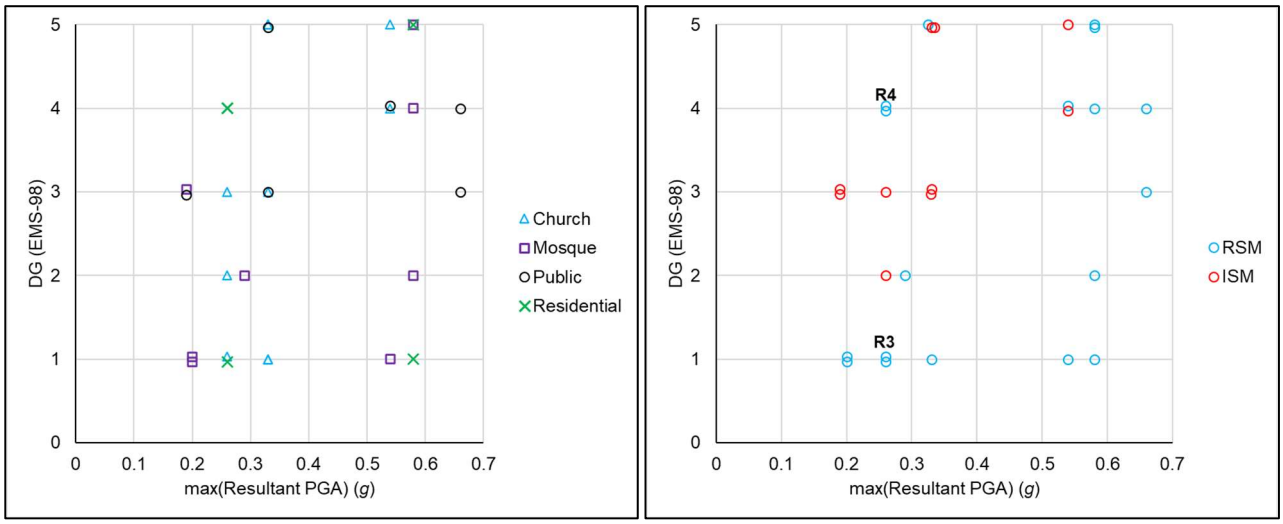

(a) (b)

Figure 2. EMS-98 DGs vs maximum resultant PGA values considering a) wall construction types b) purpose of the buildings

To understand why similar buildings may have experienced different damage levels under similar seismic demands, it is useful to examine their damage patterns. Borri et al. (2020) proposed a classification which categorises buildings according to the presence of masonry disaggregation. Masonry disaggregation refers to disintegration of walls under strong ground motions with diffuse detachment between stones and mortar. In ISM walls, disaggregation occurs when weak mortar is used alongside irregularly shaped and sized stones. In RSM walls, it typically occurs when wall leaves have weak connections and separate from each other. According to Table 1, 70% of the investigated buildings were subjected to masonry disaggregation. Masonry disaggregation is evident in how the building leaves have separated in R4 due to a lack of diatons (see Figures 3a-b); a similar separation is not observed for the building R3 in Figures 3c-d. It is thought that masonry disaggregation may have facilitated the formation of the out-of-plane collapse mechanism in R4, leading to the DG4 assignment of this building.

(a) (b)

(c) (d)

Figure 3. a) General view and b) disaggregated wall in R4 c) general view and d) a vertical crack around corner stones in R3

3. Construction technique and quality evaluation

One of the potential reasons for the out-of-plane failure of masonry walls is disaggregation. Borri et al. (2015) proposed the MQI to evaluate construction quality and judge whether a wall is prone to disaggregation.

The MQI grade is calculated using the following parameters: i) *SM*: conversation state, ii) *SD*: stone dimension, iii) *SS*: stone shape, iv) *WC*: wall-leaf connection, v) *HJ* and *VJ*: mortar joint geometry, vi) *MM*: mortar quality. A grade (e.g. fulfilled (F), partially fulfilled (PF) and not fulfilled (NF)) is assigned to each parameter and the MQI is calculated using Eq. (1):

$$MQI = SM(SD + SS + SD + WC + HJ + VJ + MM) \quad (1)$$

The weights of each parameter are determined according to the fulfilment level and the loading conditions (e.g. in-plane, out-of-plane and vertical). In this paper, the MQI for horizontal out-of-plane actions is considered. Further details about the MQI parameters (Borri et al. 2015; Borri et al. 2020) are not provided for brevity. However, Figures 4a-c are presented to show how geometric measurements were used to calculate parameters of *SD, WC* and *VJ* where the ratio of L_m/L_v is used to select the fulfilment criteria for *WC* and *VJ* (Bozyigit et al. 2023).

(a) (b) (c)

Figure 4. a) Stone dimension measurements from a point cloud for C5, b) photograph of a through thickness cross-section of a disaggregated wall used for WC calculation (Building: M1), and c) an exposed wall surface used for VJ calculation (Building: C3) (Bozyigit et al. 2023)

After calculating Eq. (1), the masonry wall is assigned a category: “A” (good quality) for 7≤ MQI ≤ 10, “B” (average quality) for 4≤ MQI ≤ 7 and “C” (poor quality) for 0≤ MQI ≤ 4. The walls categorized as “C” are prone to masonry disaggregation according to Borri et al. (2020).

Table 2 represents the MQI, the MQI category, disaggregation state and DG for the examined buildings. It should be noted that the MQI calculations were not performed for some buildings listed in Table 1 as exposed masonry surfaces and through thickness cross-sections were not available. According to Table 2, all the ISM buildings are in category “C” and disaggregation was observed for all of these, except for C4.

Half of the RSM buildings are categorized as class “B” while the rest are categorized as “C”. All class “C” RSM buildings experienced disaggregation, including R4 (see Figures 3a-b). About half of the class “B” buildings did not experience disaggregation. This includes R3 (see Figures 3c-d). However, the buildings M1, M3 and R1, which are categorised as “B”, unexpectedly experienced disaggregation. A possible reason for disaggregation in these class “B” walls, is their unfulfilled WC criteria; this indicates that their wall leaves may have separated, leading to disaggregation and out of plane collapse. An example of wall leaf separation is shown in Figure 4b and this aspect is discussed in detail elsewhere (Bozyigit et al., 2023).

Table 2. MQI value and category for walls under out-of-plane actions with disaggregation and DG data

Building	Wall construction	MQI	Category	Disaggregation	DG (EMS-98)
C2	ISM	1	C	Yes	3
C3	RSM	2.8	C	Yes	5
C4	ISM	1.4	C	No	5
C5	RSM	6	B	No	1
C6	ISM	0.35	C	Yes	3
C7	ISM	0.5	C	Yes	2
C8	ISM	1.4	C	Yes	4
C9	ISM	1.05	C	Yes	5
M1	RSM	6.5	B	Yes	5
M3	RSM	5.5	B	Yes	4
M5	ISM	1	C	Yes	3
P1	RSM	0.35	C	Yes	3
P2	ISM	0.7	C	Yes	5
P3	ISM	1	C	Yes	3
P5	ISM	0.7	C	Yes	3
P6	RSM	2.1	C	Yes	4
R1	RSM	5.5	B	Yes	5
R3	RSM	6	B	No	1
R4	RSM	2.8	C	Yes	4
R5	RSM	1.75	C	Yes	4

4. In-situ mechanical characterisation of masonry materials

The previous sections highlighted the correlation between poor wall construction quality (quantified by either MQI class “C” or unfulfilled wall-leaf connection criteria WC) and failures (disaggregation and out-of-plane collapse). To ensure that these correlations are meaningful, they need to be considered alongside the mechanical characteristics of constituent materials; disaggregation generally implies poor materials. To this end, in-situ mechanical characterization of masonry materials was conducted during the post-earthquake field work. Ultrasonic Pulse Velocity (UPV) tests were used to estimate the dynamic (E_d) and static modulus of

elasticity (E_s) of stones, Schmidt Rebound Hammer (SRH) tests were applied to estimate compressive strength of stones (f_s) and Mortar Penetrometer tests were conducted to estimate compressive strength of mortars (f_m). A brief summary of these tests are provided below. For further details, the reader is referred to Bozyigit et al. (2023).

4.1. UPV tests

UPV measurement is based on the propagation of ultrasonic waves at different velocities through materials. Proceq Pundit PI-200 device was used in the tests as follows: i) The transmitter generates the ultrasonic waves sent into the stone, ii) the receiver measures the ultrasonic waves that travelled through the stone, iii) the controller processes the signals using the time and distance that the waves travelled to obtain P-wave velocity (V_p). V_p is used to estimate the density (ρ_s) (Gardner et al. 1974) and E_d (Marazzani et al., 2021) using Eqs.(2-3), respectively.

$$\rho_s = 230 V_p^{0.25} \quad \text{(kg/m}^3\text{)} \tag{2}$$

$$E_d = \frac{\rho_s V_p^2 (1+\upsilon_s)(1-2\upsilon_s)}{(1-\upsilon_s)10^6} \quad \text{(MPa)} \tag{3}$$

where υ_s is Poisson's ratio of the stone and is assumed as 0.25.

The strain level is negligible in the ultrasonic tests. Therefore, E_d is smaller than E_s. In this study, the E_s is calculated using Eq.(4) (Eissa and Kazi, 1998):

$$E_s = 0.74 E_d - 820 \quad \text{(MPa)} \tag{4}$$

4.2. SRH tests

The Silver SRH of Proceq was used in the field work with the mushroom plunger to determine the f_s. The Silver SRH uses optical sensors to measure impact and rebound velocities. These velocities are used to obtain Q values. Ten readings were obtained for each stone sample. The average of readings are calculated to obtain Q value which is used to estimate f_s as follows (Kocáb et al., 2019):

$$f_s = 0.0108 Q^2 + 0.2236 Q \quad \text{(MPa)} \tag{5}$$

4.3. MP tests

The MP tests were performed using a device from the Diagnostic Research Company (DRC) to obtain the compressive strength of mortars. The MP device features a hammer attached to a manually loaded spring. The hammer strikes a needle when it is released and the needle is penetrates into the mortar. The hammer is struck 10 times. f_m is calculated using Eq.(6) where d_p is the penetration depth (Gambilongo et al., 2023).

$$f_m = \frac{5970 - \sqrt{(1.58 d_p - 5.3)10^6}}{1580} \quad \text{(MPa)} \tag{6}$$

The MP measurements were performed both at the surface and internally to investigate the mechanical difference in mortar for different parts of the wall.

4.4. Numerical results and discussion

In general, it was observed that a wide range of materials were used in the construction of walls, particularly in ISM and MLM walls. To provide a practical indication of the static elastic modulus and strength of materials used in each building, building-wide averages were calculated from the measurements taken across different materials located in different parts of the buildings. These are presented in Table 3 alongside disaggregation status and DGs according to EMS-98.

The building-wide average values of E_s, f_s and f_m vary between 2043-15261 MPa, 13.5-31.2 MPa and 0.5-2.4 MPa, respectively. When the average values of RSM buildings are considered, the corresponding values are 8343.3 MPa, 26.2 MPa and 1.54 MPa. For ISM buildings. they are 8770.4 MPa, 24 MPa and 1.31 MPa. These

results indicate that systematic differences did not exist between the mechanical properties of materials used in RSM and ISM buildings. From these results, it is apparent that mortar strength is uniformly low across the examined structures; it is typically less than 2 MPa.

Table 3. Estimated building-averaged E_s, f_s and f_m values of the buildings with construction type, disaggregation status and DGs

Building	Wall construction	E_s (MPa)	f_s (MPa)	f_m (MPa)	Disaggregation	DG (EMS-98)
C3	RSM	8726	13.5	2.1	Yes	5
C4	ISM	11538	18.5	1.2	No	5
C5	RSM	7956.4	24.1	n/a	No	1
C6	ISM	10553.8	26.2	2.4	Yes	3
C7	ISM	14461	23.5	1.45	Yes	2
C8	ISM	7645.6	25.2	0.95	Yes	4
C9	ISM	8578	26.1	2	Yes	5
M1	RSM	15260.2	26.9	1	Yes	5
M2	RSM	3398	22.2	n/a	No	1
M3	RSM	6506	26.5	n/a	Yes	4
M4	RSM	11604.6	28.5	2.2	Yes	2
M5	ISM	6128.6	25.9	0.9	Yes	3
M6	RSM	2043.8	28.2	1.35	No	2
M7	RSM	5114.8	27.4	n/a	No	1
P1	RSM	7690	28.6	0.6	Yes	3
P2	ISM	6787.2	24.7	0.5	Yes	5
P3	ISM	4471	21.8	1.05	Yes	3
R1	RSM	8859.2	28.6	1.15	Yes	5
R2	RSM	8755.6	31.2	n/a	Yes	1
R3	RSM	8407.8	28	1.3	No	1
R4	RSM	12041.2	31	2	Yes	4
R5	RSM	10442.8	21.7	2.2	Yes	4

Table 3 does not show any apparent trends between the mechanical properties of masonry constituents and DG levels. This observation indicates that the construction quality may have been the dominant aspect governing the out-of-plane failures of masonry walls. In particular, for RSM walls, the inter-leaf wall connections appear to have had a dominant role in the failure. On the other hand, past earthquake observations (Decanini et al. 2002) indicated that mortar may have a strong influence on the resistance of ISM walls against disaggregation and out-of-plane collapse. Low mortar strength of the examined buildings may have facilitated disaggregation in the examined ISM structures. The fact that all ISM structures, even those with the lowest PGA, experienced disaggregation corroborates this statement.

5. Conclusions

This paper surveyed the damage, evaluated construction quality and discussed in-situ material characterisation of the walls of 29 monumental stone masonry buildings in Hatay and Osmaniye after 2023 Turkey-Syria earthquakes. The concluding remarks are listed below:

- In general, regular stone masonry constructions experienced less damage than irregular stone masonry constructions when subjected to similar peak ground accelerations.
- Masonry disaggregation was observed in 70% of the investigated buildings. This observation indicated poor construction quality and materials.

- The Masonry Quality Index was calculated for 20 buildings based on wall leaf, stone and mortar geometries. 75% of these buildings was categorised as class “C”, which indicates poor construction quality prone to disaggregation. A strong correlation was found between the MQI category “C” and the presence disaggregation amongst the investigated buildings.
- Some buildings which were associated with average MQI quality class “B” also experienced disaggregation. It was observed that these walls had poor inter-leaf connection, which caused the walls to disaggregate.
- The elastic modulus and compressive strength of stones vary between 2043-15261 MPa, 13.5-31.2 MPa, respectively. These ranges show that a wide variety of stones were used for the walls of the monumental buildings in the area.
- The compressive strength of mortars range between 0.5-2.4 MPa. These values indicate low strength and help explain why disaggregation was common in ISM walls, even for low seismic demands.

Acknowledgements

The field work conducted as a part of this study was supported by EPSRC (via the grants EP/P025641/1 and EP/V048082/1) and TUBITAK (2221-Fellowships for Visiting Scientists and Scientists on Sabbatical Leave Support Programme). Earthquake Engineering Field Investigation Team (EEFIT) organised the first field mission. Baran Bozyigit acknowledges the financial support of TUBITAK 2219-International Postdoctoral Research Fellowship Programme. The authors would like to thank Shirley Underwood from Screening Eagle/Proceq for the loan of NDT equipment used in this research. Thanks are also due to DRC Italia for supplying equipment at short notice. FARO UK provided free software licenses to enable laser scan data processing –University of Oxford DPhil students Yilong Yang, Yixiong Jing and Zheng-You Zhang provided the processed data. The authors are grateful to building owners and custodians for allowing them access; the list is too long to acknowledge here but special thanks are due to Yusuf Tabasyan (Iskenderun Karasun Manuk Church), Ratibe Bugrahan (Hatay Metropolitan Municipality) Gokhan Cicek (Directorate of Foundations), Abdullah Papas (St George Sarilar Orthodox Church) and Dimyan Emektas (St Ilyas Orthodox Church). Logistic help from Misel Uyar (Nehna) and Ahmet Cakmak (Istanbul Metropolitan Municipality) made this work possible. We also acknowledge our academic collaborators, Prof. Heather Viles, Prof. Alper Ilki, Prof. Bora Pulatsu, Prof. Eser Cakti, Prof. Paulo Lourenço and Dr Pascal Lava for contributing in various ways to this study.

6. References

AFAD (2023) Turkish Ministry of Interior Disaster and Emergency Management Presidency.

Borri A, Corradi M, Castori G and De Maria A (2015) A method for the analysis and classification of historic masonry. *Bulletin of Earthquake Engineering*, 13: 2647-2665.

Borri A, Corradi M and De Maria A (2020) The Failure of Masonry Walls by Disaggregation and the Masonry Quality Index. *Heritage*, 3(4): 1162-1198.

Bozyigit, B., Ozdemir, A., Donmez, K., Dalgic, K.D., Durgut, E., Yesilyurt, C., Dizgin, Y., Yıldeniz, C., Ispir, M., Bedirhanoglu, I., Aktas, Y.D., Acikgoz, S. (2023) Damage to monumental masonry buildings in Hatay and Osmaniye following the 2023 Turkey-Syria earthquakes: the role of wall geometry, construction quality and material properties, *Earthquake Spectra*, Under Review.

Decanini, L., De Sortis, A., Goretti, A., Langenbach, R., Mollaioli, F., Rasulo, A. (2004) Performance of masonry buildings during the 2002 Molise, Italy, Earthquake. *Earthquake Spectra*, 20(1_suppl), 191-220.

Eissa EA and Kazi A (1988) Relation between static and dynamic Young's moduli of rocks. *International Journal of Rock Mechanics and Mining Sciences*, 25(6): 479-482.

Gambilongo L, Barontini A, Silva RA and Lourenço PB (2023) Evaluation of non-destructive techniques for mechanical characterisation of earth-based mortars in masonry joints. *Construction and Building Materials*, 392: 131960.

Gardner G, Gardner L and Gregory A (1974) Formation velocity and density—The diagnostic basics for stratigraphic traps. *Geophysics*, 39(6): 770-780.

Grünthal G and Levret A (1998) European macroseismic scale 1998 (EMS-98) cahiers du centre Européen de géodynamique et de séismologie 15. Centre Européen de géodynamique et de séismologie, Luxembourg.

Kocáb D, Misák P and Cikrle P (2019) Characteristic curve and its use in determining the compressive strength of concrete by the rebound hammer test. *Materials*, 12(17): 2705.

Marazzani J, Cavalagli N and Gusella V (2021) Elastic properties estimation of masonry walls through the propagation of elastic waves: An experimental investigation. *Applied Sciences*, 11(19): 9091.

Mavroulis S, Andreadakis E, Spyrou N-I, Antoniou V, Skourtsos E, Papadimitriou P, Kasssaras I, Kaviris G, Tselentis GA, Voulgaris N, Carydis P and Lekkas E (2019) UAV and GIS based rapid earthquake-induced building damage assessment and methodology for EMS-98 isoseismal map drawing: The June 12, 2017 Mw 6.3 Lesvos (Northeastern Aegean, Greece) earthquake. *International Journal of Disaster Risk Reduction*, 37: 101169.

Ozkula, G., Dowell, R. K., Baser, T., Lin, J. L., Numanoglu, O. A., Ilhan, O., Olgun, C. G, H, C. W., Uludag, T. D. (2023). Field reconnaissance and observations from the February 6, 2023, Turkey earthquake sequence, *Natural Hazards*, 1-38.

USGS (2023) U.S. Geological Survey. Earthquake Lists, Maps, and Statistics, accessed July 13, 2023 at URL https://www.usgs.gov/natural-hazards/earthquake-hazards/lists-maps-and-statistics.